Structures, Energetics, and Reactions of $[C_2H_3S]$ Radicals and $[C_2H_3S]^+$ Ions: A Gaussian-2 ab Initio Study

S.-W. Chiu*

Department of Molecular and Integrative Physiology and Beckman Institute for Advanced Studies, University of Illinois, 405 N. Mathews, Urbana, Illinois 61801

Kai-Chung Lau† and Wai-Kee Li*

Department of Chemistry, The Chinese University of Hong Kong, Shatin, N.T., Hong Kong

Received: November 18, 1999; In Final Form: January 21, 2000

A detailed computational study on the structures, energetics, and reactions of the isomers of the $[C_2H_3S]$ radical and the $[C_2H_3S]^+$ cation has been carried out. The computational models used are slightly modified versions of the ab initio Gaussian-2 method. Ten $[C_2H_3S]$ isomers have been identified. Among them, the thioformylmethyl radical (**1**) has the lowest energy, with a ΔH_{f0} value of 214 kJ mol^{-1}. Other more chemically important isomers include the thioacetyl radical (**2**), thiiranyl radical (**4**), 1-thiovinyl radical (**8**), and 2-thiovinyl radical (**11**, **12**, **13**, **14**); the ΔH_{f0} values for these isomers are 251, 301, 314, and 342−347 kJ mol^{-1}, respectively. In addition, we have also studied various reactions involving these radicals. For instance, it is found that isomerization reactions of **1** to **2**, **4**, **8**, and **12** have barriers ranging from 123 to 227 kJ mol^{-1}. On the other hand, reaction **2** → **3** proceeds via a dissociation/recombination mechanism: **2** → CS + CH_3 → **3**. The dissociation process is the rate-determining step, with a barrier of 187 kJ mol^{-1}. On the $[C_2H_3S]^+$ potential energy surface, 12 isomers have been found. Among them, $\mathbf{2}^+$ has the lowest energy, with a ΔH_{f0} value of 891 kJ mol^{-1}. Other isomers with ΔH_{f0} values within 200 kJ mol^{-1} of that of $\mathbf{2}^+$ include $\mathbf{8}^+$, $\mathbf{4}^+$, $\mathbf{5}^+$, $\mathbf{1}_t^+$ (triplet state of $\mathbf{1}^+$), and S-protonated ethynylthiol ($\mathbf{16}^+$). Reactions involving these cations studied in this work include: $\mathbf{4}^+ \rightarrow \mathbf{2}^+$ (barrier being 116 kJ mol^{-1}) and $\mathbf{4}^+ \rightarrow \mathbf{8}^+$ (152 kJ mol^{-1}), both having $\mathbf{1}^+$ as the transition structure; 1,2-H shift reaction $\mathbf{4}^+ \rightarrow \mathbf{5}^+$ (219 kJ mol^{-1}); 1,3-H shift reaction $\mathbf{8}^+ \rightarrow \mathbf{16}^+$ (232 kJ mol^{-1}); $\mathbf{8}^+ \rightarrow \mathbf{2}^+/\mathbf{4}^+$ (162 kJ mol^{-1}); and $\mathbf{8}^+ \rightarrow \mathbf{5}^+$ (171−175 kJ mol^{-1}) with two distinct pathways. The ΔH_{f0} values for various species calculated in this work are in good accord with available experimental measurements. Furthermore, the kinetics data reported here for reactions involving $[C_2H_3S]^+$ cations are consistent with the results obtained in low-energy collision activated dissociation experiments.

1. Introduction

There have been only a few experimental[1−5] and theoretical[6−11] studies on the structures, energetics, isomerization, and fragmentation of $[C_2H_3S]^+$ ions. Despite these activities, thermochemical data for $[C_2H_3S]^+$ ions remain very sparse.[12,13] To our knowledge, no up-to-date experimental or theoretical investigations other than the study[14] of thioformylmethyl radical (CH_2-CHS), along with other substituted allyl radicals, on $[C_2H_3S]$ isomers are available.[12,13] In this work, we investigate theoretically the structures and energetics of various $[C_2H_3S]$ isomers as well as the pathways of their isomerization reactions. In addition, we revisit the structures and energetics of $[C_2H_3S]^+$ ions and their rearrangements. Previous theoretical studies of $[C_2H_3S]^+$ ions were restricted to the Hartree−Fock (HF) level and included only a limited number of $[C_2H_3S]^+$ isomers.[6−11] It is therefore desirable to undertake a more systematic study for the $[C_2H_3S]^+$ isomers and their isomerization and fragmentation pathways at a higher theoretical level. Such information would allow for a reliable interpretation of the collision-activated dissociation (CAD) spectra[3,5] of these ions.

2. Theoretical Method

The computational method employed in this work is the same as those used in our previous studies on $[C_2H_5S]^+$ ions.[15,16] The Gaussian-2 (G2) procedure[17] was used to obtain the G2 energies of the molecular systems studied in this work. Structural optimizations and frequency calculations were performed at the QCISD/6-31(d) level. Population analyses were carried out at the same theoretical level. For some structures, these calculations were also performed at the QCISD/6-311G(d,p) or CCSD/6-31G(d) level. All electrons were included in the calculation of correlation energies for all post-HF optimizations and frequency calculations. The scaling factor (0.95)[16] for QCISD/6-31G(d) frequencies was used to scale all post-HF frequencies in calculations of zero-point energies (ZPE) and thermal corrections. All transition-state (TS) structures except rotational TSs were characterized by intrinsic reaction coordinate (IRC) calculations at the QCISD/6-31G(d) level unless otherwise stated explicitly.

In this work, single- or double-digit numerals such as **1**, **2**, ..., etc., refer to the structures of $[C_2H_3S]$ radicals and numerals with superscript + such as $\mathbf{1}^+$, $\mathbf{2}^+$, ..., etc. refer to the structures of singlet $[C_2H_3S]^+$ ions derived from radicals **1**, **2**, ..., etc., respectively. Their corresponding triplet states are designated

† Present address: Department of Chemistry, Iowa State University, Ames, IA 50011.

10.1021/jp9941054 CCC: $19.00
Published on Web 03/10/2000

as $\mathbf{1}_t^+$, $\mathbf{2}_t^+$, ..., etc. In addition, notation such as $\mathbf{1}-\mathbf{2}^+$ refers to the TS structure connecting $\mathbf{1}^+$ and $\mathbf{2}^+$.

In this work, we carried out stability test for all the zeroth-order, or HF reference, wave functions of all the optimized structures. Some of the $[C_2H_3S]^+$ isomers and TS structures with open-shell character had unstable restricted HF (RHF) functions, i.e., allowing the RHF determinant to become unrestricted (UHF) leads to a lower energy solution. Such *problematic* systems have been discussed previously.[15,16] Molecular systems thought to be closed-shell species having RHF instability were also reoptimized at the UQCISD/6-31G(d) level with the optimized UHF reference wave functions as initial guess and subsequent single-point calculations for G2 energies were carried out with the UHF formalism. We denote, for example, $G2_{UQCISD}$ energies as G2 energies calculated at UQCISD/6-31G(d) optimized structures with the UHF formalism. Similarly, $G2_{RQCISD}$ denotes G2 energies calculated at RQCISD/6-31G(d) optimized structures with the RHF formalism. In general, when the *singlet* is the true ground state for such a problematic system, its $G2_{RQCISD}$ energy is consistent with the $G2_{UQCISD}$ results.[15,16,18] On the other hand, in the regions of the potential energy surface (PES) having a triplet ground state, RHF functions for singlet states are always unstable and calculations based on unrestricted methods would give a poor approximation to the triplet energy.[19]

Unless stated otherwise, calculated energies and thermochemical properties reported in this work refer to 0 K at the $G2_{QCISD}$ level ($G2_{UQCISD}$ for open-shell and $G2_{RQCISD}$ for closed-shell systems). For open-shell systems, energy correction for spin contamination is approximated by $\Delta E_{cor} = E(\text{PMP4/6-311G(2df,p)}) - E(\text{UMP4/6-311G(2df,p)})$.[20] However, calculated energies with spin-contamination correction (SCC) according to this simple scheme may not be necessarily better than the uncorrected values[20,21] at least due to structures not optimized with respect to spin-projected wave functions. We denote G2 energies with SCC as PG2 energies. Throughout this paper, we use the uncorrected values for discussion except where stated otherwise.

3. Results and Discussion

There exist at least 10 $[C_2H_3S]$ isomers, as shown in Figure 1. Figure 2 illustrates the $[C_2H_3S]$ TS structures. The $G2_{UQCISD}$ energies and calculated heats of formation (ΔH_{f0}) of these structures are summarized in Table 1. Table 2 lists the same information for $[C_2H_3S]^+$ ions and other related molecular species. Equilibrium and TS structures of $[C_2H_3S]^+$ ions are presented in Figures 3 and 4, respectively. Figures 5 and 6 illustrate the PESs of the $[C_2H_3S]$ radicals and the $[C_2H_3S^+]$ ions, respectively.

3.1. Structures and Energetics of $[C_2H_3S]$ and $[C_2H_3S]^+$ Isomers. *3.1.1. Thioformylmethyl Radical (1) and Cation (1^+).* Among the $[C_2H_3S]$ radicals studied in this work, **1** has the lowest energy. Its calculated ΔH_{f0} is 214 kJ mol^{-1}. This radical is isoelectronic (inner-shell electrons ignored) with the allyl radical, whose automerization path, vibrational modes, and rotational energy barriers (ΔE_b) have been studied at various theoretical levels.[22] Results of a natural bond orbital (NBO)[23] analysis indicate that there is hyperconjugation between the radical orbital (n_π(S)) and the π(C−C)/π^*(C−C) orbitals. The consequences of these orbital interactions are (i) weakening and hence lengthening of the C−C bond; (ii) strengthening and hence shortening of the C−S bond due to partial π bonding between the two atoms; and (iii) stabilizing n_π(S) so that the highest occupied molecular orbital (HOMO) corresponds to one of the nonbonding orbitals n_σ(S). The C−S bond length (1.711 Å) is shorter than that (1.81 Å) of paraffinic thiols such as CH_3-SH and its C−C bond length (1.366 Å) is slightly longer than a typical C−C double bond (1.34 Å). We found α-spin densities at the terminal C (0.52) and S (0.79) atoms and β-spin density (−0.26) at the central C atom of **1**, in agreement with the results of Wiberg et al.[14] The interaction of the unpaired α-spin electron with the two π bonding electrons must involve spin polarization and cause a small net β-spin density at the central C atom.[22] Rotation of the methylene group about the C−C bond is restricted due to a large ΔE_b of 89 kJ mol^{-1}. By comparison the rotational barrier[14] for CH_2CHCH_2 is 64 kJ mol^{-1} at the G2(MP2)[24] level. The higher-energy rotational barrier for **1** than CH_2CHCH_2 is attributed to the preference of the odd electron going to the less electronegative atom,[14] leading to a more localized and stronger π(C−C) bond. The rotational TS (**1a**)

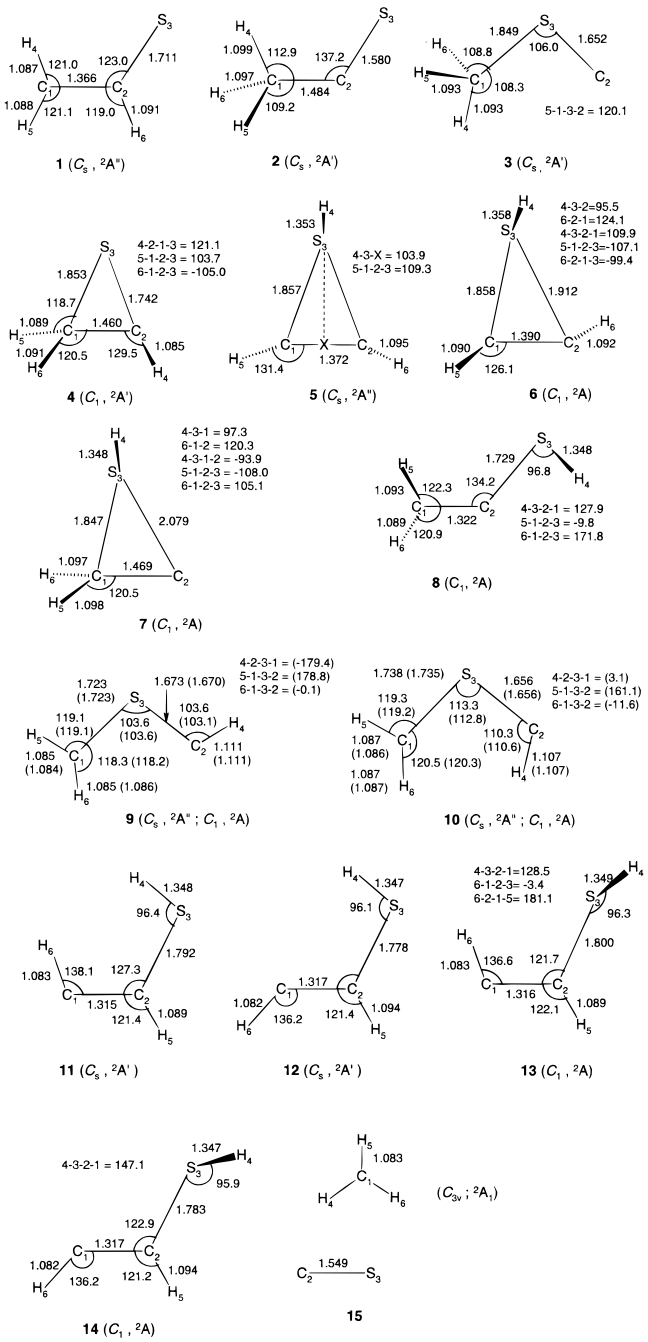

Figure 1. $[C_2H_3S]$ structures optimized at the UQCISD/6-31G(d) level. For **9** and **10**, numbers in parentheses are for their C_1 structures.

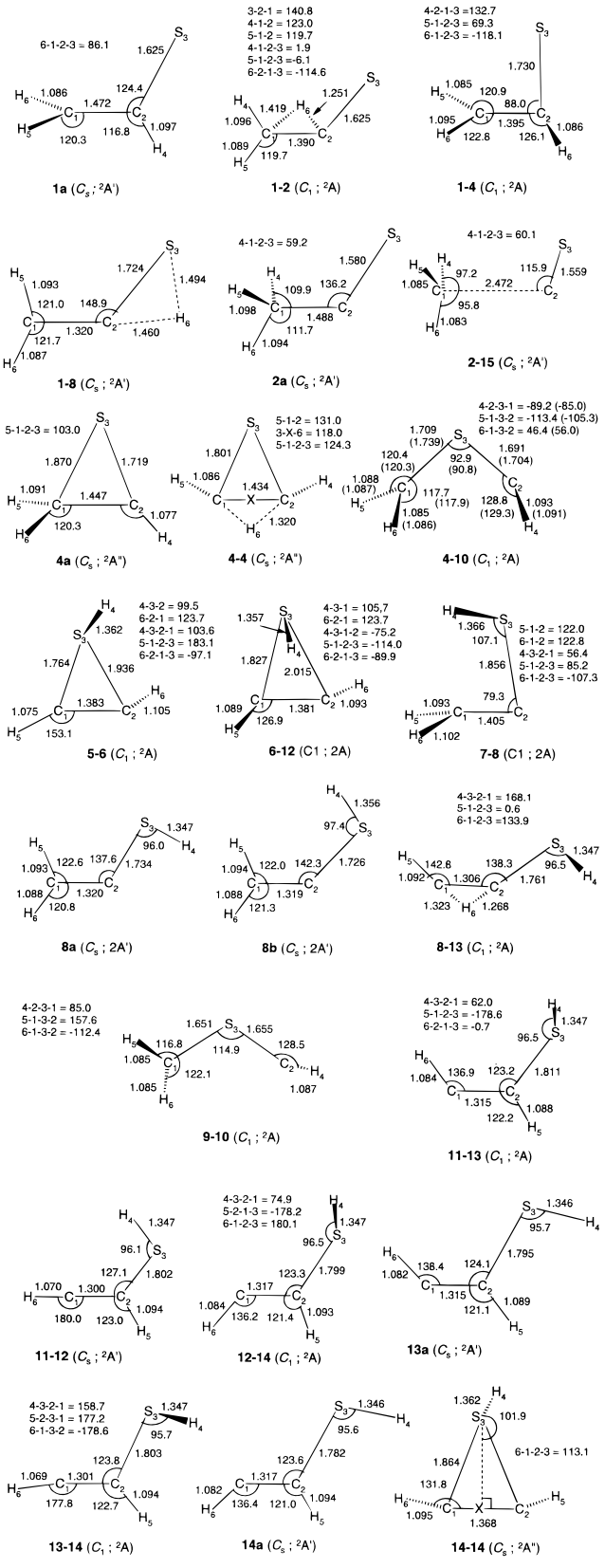

Figure 2. Transition-state structures for $[C_2H_3S]$ radicals optimized at the UQCISD/6-31G(d) level. For TS **4**−**10**, the values in parentheses were calculated with the unstable UHF/6-31G(d) function as zeroth-order reference wave function.

has longer C−C bond length (1.472 Å) than **1** because of the rupture of the π(C−C) bond. However, its C−S bond now has double bond character (1.624 Å). The C atom of the rotating CH_2 group has an α-spin density of 1.16 while the S and the central C atoms have α- and β-spin densities of 0.09 and −0.14, respectively. In both conformations, spin polarization is the dominant mechanism for the interaction of the spin of the unpaired electron with the paired electrons.[22]

Previous theoretical calculations[6,8,10] on $\mathbf{1}^+$ were based on the RHF formalism. The closed-shell singlet (^{1}A′) formally has its lowest unoccupied molecular orbital with π symmetry centered on the S atom and is isoelectronic with the allyl cation which has been generated[25] in a superacid cryogenic matrix. In the CAD study of $[C_2H_3S]^+$ ions,[3] $\mathbf{1}^+$ was postulated as a plausible structure of $[C_2H_3S]^+$ ions. That the formally singly occupied orbital, n_π(S), of **1** is not the HOMO suggests that $\mathbf{1}^+$ would be formed preferentially by removal of one of the n_σ(S) electrons of **1**, resulting in an open-shell structure which can be either triplet (^{3}A″) or singlet (^{1}A″). Since favorable exchange interactions in the triplet are absent in the open-shell

TABLE 1: G2 Electronic Energies E_e (hartrees), Zero-Point Energies ZPE (millihartrees), Thermal Corrections $H_{298} - H_0$ (millihartrees), and Enthalpies of Formation at 0 K ΔH_{f0} (kJ mol^{-1}) for $[C_2H_3S]$ Radicals and Other Related Molecular Species

				ΔH_{f0}		
species	E_e	ZPE	$H_{298} - H_0$	$G2_{UQCISD}$	$PG2_{UQCISD}$	$\langle S^2 \rangle$
1	−475.575 60	40.23	5.08	214.1	188.1	0.975
2	−475.561 71	40.23	5.08	250.5	231.5	0.948
3	−475.492 59	38.61	4.90	427.8	422.1	0.773
4	−475.542 77	40.48	4.33	300.9	296.4	0.767
5	−475.463 83	35.93	4.75	496.2	490.2	0.780
6	−475.464 72	35.88	4.89	493.8	487.4	0.780
7	−475.458 74	36.44	4.94	510.9	506.6	0.766
8	−475.453 09	36.95	5.17	313.9	290.9	0.988
9 (C_1)	−475.476 71	36.04	5.16	462.7	441.1	1.091
9 (C_s)	−475.476 72	36.01	5.12	462.6	452.9	0.789
10 (C_1)	−475.472 69	35.45	5.39	471.7	448.4	1.096
10 (C_s)	−475.472 50	35.36	5.45	472.0	461.4	0.797
11	−475.523 09	36.36	5.19	341.8	316.8	1.008
12	−475.522 40	36.16	5.17	343.1	318.9	1.004
13	−475.522 33	36.31	5.26	343.7	319.9	1.000
14	−475.521 06	36.00	5.29	346.2	322.2	1.004
1a	−475.538 46	37.07	4.78	303.3	275.3	1.087
2a	−475.561 71	39.86	4.37	252.4	226.1	0.966
3a	−475.491 92	38.39	4.57	429.0	421.7	0.774
4a	−475.537 62	38.87	4.24	310.2	305.0	0.771
8a	−475.530 16	35.88	4.78	322.0	299.5	0.980
8b	−475.527 91	35.52	4.81	326.9	304.8	0.976
13a	−475.521 97	35.89	4.65	343.5	318.5	1.011
14a	−475.521 38	35.66	4.66	344.4	319.9	1.009
1−**2**	−475.496 75	35.68	4.60	409.2	404.6	0.771
1−**4**	−475.527 90	39.34	4.20	337.0	306.0	1.076
1−**8**	−475.487 37	32.77	5.29	429.0	397.9	1.016
1−**12**	−475.482 05	33.12	4.62	441.0	405.8	1.087
2−**15**	−475.483 84	33.75	6.20	438.0	423.0	0.857
3−**15**	−475.478 93	35.31	5.61	455.0	428.2	0.972
4−**4**	−475.447 33	34.69	4.37	536.3	526.6	0.812
4−**10**	−475.442 26	35.27	4.80	551.1	520.8	1.678
4−**10**[a]	−475.451 50	35.66	4.68	527.9	522.4	0.788
5−**6**	−475.455 48	34.27	4.61	513.8	508.9	0.773
6−**12**	−475.464 28	35.20	4.47	493.2	485.7	0.790
7−**8**	−475.449 38	34.94	4.60	531.6	528.2	0.762
8−**13**	−475.453 09	30.96	5.29	511.4	503.3	0.800
9−**10**[a]	−475.466 04	35.38	4.86	489.0	483.0	0.784
11−**12**	−475.516 35	34.30	5.16	354.1	328.3	0.989
11−**13**	−475.520 81	35.96	4.63	346.7	321.3	1.016
12−**14**	−475.518 11	35.62	4.65	352.9	328.5	1.010
13−**14**	−475.515 42	34.08	5.34	355.9	330.3	0.990
14−**14**	−475.462 09	34.21	4.61	496.3	489.4	0.787
$\mathbf{CH_3}$	−39.772 71	28.51	4.09	151.9 147 ± 1[b]	148.8	0.762
CS	−435.713 89	2.78	3.32	272.4 280.3284[c]		

[a] Calculations based on UHF-unstable zero-order reference wave function. [b] Experimental ΔH_{f298} value. References 13 and 55. [c] Experimental ΔH_{f298} value. References 13 and 54.

TABLE 2: G2 Electronic Energies E_e (hartrees), Zero-Point Energies ZPE (millihartrees), Thermal Corrections $H_{298} - H_0$ (millihartrees), and Enthalpies of Formation at 0 K ΔH_{f0} (kJ mol^{-1}) for $[C_2H_3S^+]$ Ions and Other Related Molecular Species

species	E_e[a]	ZPE[a]	$H_{298} - H_0$[a]	ΔH_{f0} G2[a]	ΔH_{f0} PG2	$\langle S^2 \rangle$	method
$\mathbf{1}_t^+$	−475.242 01	39.21	4.71	1087.2	1071.4	2.151	
$\mathbf{1}^+$	−475.230 48	45.32	4.33	1133.6			
	−475.230 48	39.94	4.30	1119.4			$G2_{RCCSD}$
	−475.229 23	40.99	5.10	1125.5			$G2_{RCISD}$
	−475.237 22	39.73	4.74	1101.2	1094.8	1.070	$G2_{UQCISD}$
$\mathbf{1}-\mathbf{2}^+$	−475.224 71	35.28	4.75	1122.4			
	−475.211 13	35.95	4.62	1159.8	1118.4	0.905	$G2_{UQCISD}$
$\mathbf{1}-\mathbf{4}^+$	−475.230 13	40.89	4.26	1122.9			$G2_{RCISD}$
	−475.234 58	39.42	4.25	1107.3	1074.8	0.918	$G2_{UQCISD}$
$\mathbf{1}-\mathbf{8}^+$	−475.208 67	33.03	5.33	1158.6			
	−475.203 8	33.02	5.40	1171.3	1109.4	0.689	$G2_{UQCISD}$
$\mathbf{2}^+$	−475.318 72	40.97	4.76	890.5			
	−475.318 07	41.07	4.75	892.4 (879)[b,4] (853)[b,12]	882.8	0.082	$G2_{UQCISD}$
$\mathbf{2}-\mathbf{3}^+$	−475.180 06	37.83	4.96	1246.3			
$\mathbf{3}^+$	−475.187 48	38.92	5.27	1229.7			
$\mathbf{3a}^+$	−475.183 88	38.49	4.80	1238.0			
$\mathbf{3}-\mathbf{4}^+$	−475.182 02	36.46	4.27	1237.5			
$\mathbf{4}^+$	−475.274 57	41.04	4.34	1006.6			
	−475.274 08	41.33	4.32	1008.6	990.0	0.183	$G2_{UQCISD}$
$\mathbf{4}-\mathbf{5}^+$	−475.184 00	34.06	4.59	1226.0			
	−475.182 13	34.25	4.57	1231.5	1201.2	0.356	$G2_{UQCISD}$
$\mathbf{4}-\mathbf{7}^+$	−475.155 46	34.81	4.51	1302.9			
	−475.154 62	34.93	4.50	1305.5	1276.5	0.450	$G2_{UQCISD}$
$\mathbf{4}-\mathbf{9}^+$	−475.161 15	36.65	4.49	1292.8			$G2_{RCCSD}$
	−475.162 97	37.97	4.36	1291.5			$G2_{RCISD}$
	−475.159 23	35.40	4.95	1294.6	1253.8	1.196	$G2_{UQCISD}$
$\mathbf{5}^+$	−475.258 92	38.01	4.58	1039.7			
$\mathbf{5}-\mathbf{8a}^+$	−475.207 39	34.83	4.91	1166.7			$G2_{RQCISD}$[c]
$\mathbf{5}-\mathbf{8b}^+$	−475.205 32	34.78	4.84	1172.0			$G2_{RQCISD}$[c]
$\mathbf{5}-\mathbf{12}^+$	−475.207 44	34.98	4.91	1166.9			
$\mathbf{5}-\mathbf{14}^+$	−475.205 35	34.95	4.84	1172.3			
$\mathbf{7}^+$	−475.173 83	36.57	4.73	1259.3			
	−475.171 30	36.51	4.74	1265.8	1241.3	0.460	$G2_{UQCISD}$
$\mathbf{7}-\mathbf{8}^+$	−475.167 66	35.85	4.44	1273.6			
	−475.165 46	35.81	4.45	1279.3	1249.0	0.472	$G2_{UQCISD}$
$\mathbf{8}^+$	−475.275 00	37.59	5.01	996.4			
$\mathbf{8a}^+$	−475.223 24	34.06	5.11	1123.0			
$\mathbf{8b}^+$	−475.219 16	32.10	5.61	1128.6			$G2_{RQCISD}$[c]
$\mathbf{8c}^+$	−475.217 51	32.80	5.31	1134.7			
$\mathbf{8}-\mathbf{16}^+$	−475.180 68	31.67	5.27	1228.5			
	−475.179 17	31.98	5.27	1233.3	1200.7	0.244	
$\mathbf{9}^+$	−475.158 86	36.77	5.26	1299.1			
	−475.170 41	36.39	5.14	1267.8	1254.7	1.186	$G2_{UQCISD}$
$\mathbf{9}_t^+$	−475.174 98	37.00	4.98	1257.4	1231.0	2.316	
$\mathbf{9}_t-\mathbf{10}_t^+$	−475.167 70	34.53	5.22	1270.1	1241.5	2.317	
$\mathbf{10}_t^+$	−475.171 07	36.73	5.03	1267.0	1240.8	2.318	
$\mathbf{12}^+$	−475.207 83	34.76	5.64	1165.3			
$\mathbf{14}^+$	−475.209 82	34.50	5.65	1159.4			
$\mathbf{16}^+$	−475.236 88	36.21	5.36	1092.9			
$\mathbf{16}-\mathbf{17}^+$	−475.151 90	33.87	4.93	1309.8			
$\mathbf{16}-\mathbf{18}^+$	−475.141 63	31.17	5.34	1329.7			
$\mathbf{17}^+$	−475.157 91	34.91	5.43	1296.8			
	−475.157 10	34.89	5.45	1298.8	1275.5	0.358	$G2_{UQCISD}$
$\mathbf{17}-\mathbf{18}^+$	−475.149 26	34.42	4.76	1318.2			
	−475.151 51	34.41	4.76	1312.2	1288.5	0.373	$G2_{UQCISD}$
$\mathbf{18}^+$	−475.158 21	35.18	5.29	1296.7			
	−475.155 96	35.16	5.30	1302.5	1279.0	0.365	$G2_{UQCISD}$
HCC	−76.488 44	13.94	3.90	572.9 (556 ± 8)[b,13,55] (476.976)[b,13,54]	531.3	1.194	
HCC^-	−76.600 74	13.61	3.75	277.1			
$HCCH^+$	−76.791 27	24.52	3.88	1334.3	1.3	0.754	
H_2S^+	−398.562 01	14.24	3.80	988.4			

[a] $G2_{RQCISD}$ values unless otherwise stated explicitly. [b] Experimental ΔH_{f298} value. [c] Calculation based on RQCISD/6-311G(d,p) structure and frequencies.

singlet, the former state is usually lower in energy.[26] Nevertheless, violation of Hund's rule[27] have been predicted to be possible for diradicals in which the two nonbonding MOs are confined to disjoint sets of atoms.[26] We found that $\mathbf{1}_t^+$ is 46 kJ

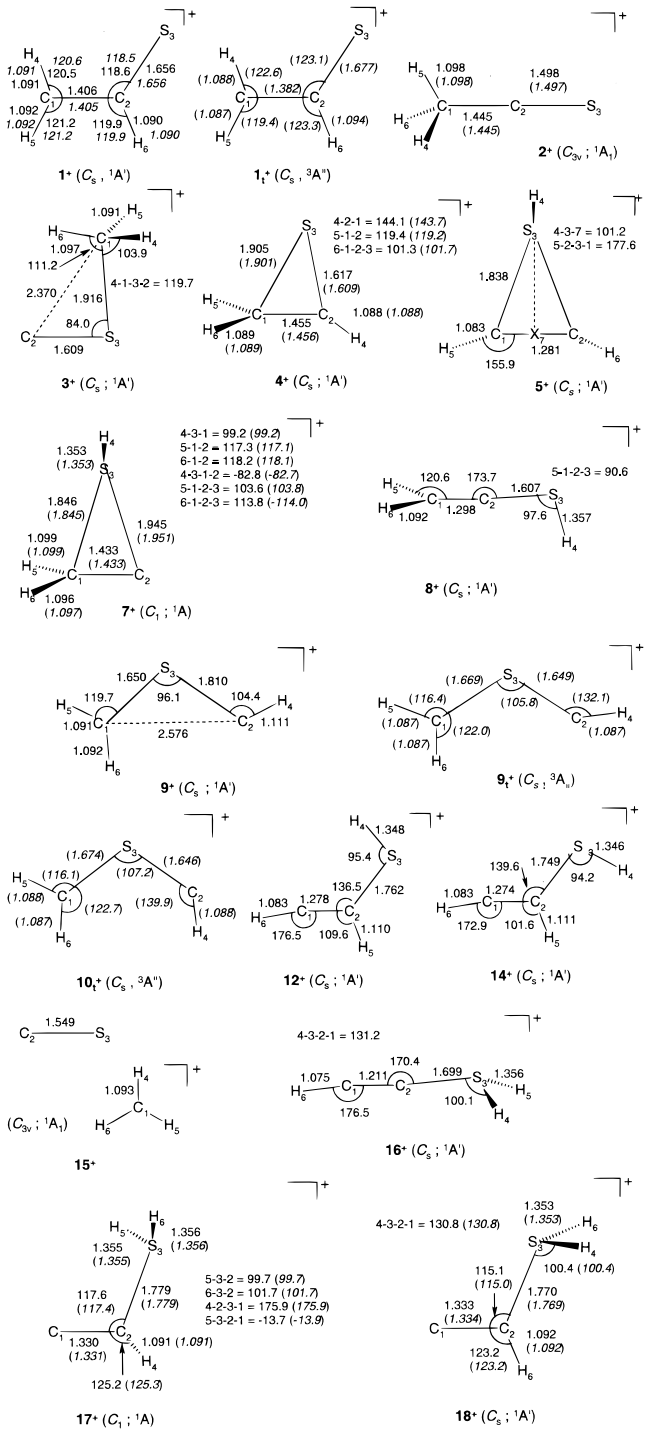

Figure 3. $[C_2H_3S]^+$ structures optimized at the RQCISD/6-31G(d), UQCISD/6-31G(d) (italic numbers in parentheses), and RCCSD/6-31G(d) (italic numbers) levels.

mol^{-1} lower in energy than $\mathbf{1}^+$. The latter has its RHF function unstable on conversion to UHF function which has A″ symmetry and has $\langle S^2\rangle$ value close to 1. This UHF function, formally corresponding to ^{1}A″ state, is essentially a mixture of singlet and triplet states. Thioformylmethyl cation, CH_2, and O_2 share a common feature: they all have triplet ground state and RHF-unstable functions for their closed-shell structures. At the $G2_{UQCISD}$ level, $\mathbf{1}^+(^1A'')$ was found only 14 kJ mol^{-1} above $\mathbf{1}_t^+$. Using CH_2 and O_2 as examples, Davidson and co-workers have illustrated that in regions of the PES having a triplet ground state, unrestricted calculations for open-shell singlet produces a poor approximation to the triplet energy and RHF calculations are always unstable.[19] Nevertheless, the G2[17] and Gaussian-3[28] ΔH_{f298} values for $CH_2(^1A_1)$, based on RHF-unstable reference wave functions, are still in good agreement with experimental values. Our complete active space self-consistent field[29,30] calculations using 8 electrons and 8 orbitals in the active space place $\mathbf{1}^+$ and $\mathbf{1}^+(^1A'')$ 49 and 79 kJ mol^{-1}, respectively, above $\mathbf{1}_t^+$. The former singlet−triplet energy separation (E_{ST}) is consistent with the $G2_{QCISD}$ result (46 kJ mol^{-1}). At the $G2_{RQCISD}$ level, $\mathbf{1}^+$ is 243 kJ mol^{-1} higher in energy than CH_3-CS^+ ($\mathbf{2}^+$).

We note that $\mathbf{1}^+$ does not correspond to a local minimum at the RMP2/6-31G(d) and RCCSD/6-31G(d) levels but to a stationary point with one imaginary frequency. As discussed in section 3.3.1 in more detail, $\mathbf{1}^+$ may either be in a very shallow potential-energy well or is a TS structure. Either way, it is an important transient species involved in the interconversions among $\mathbf{2}^+$, $\mathbf{4}^+$, and $\mathbf{8}^+$.

3.1.2. Thioacetyl Radical (2), Isothioacetyl (3), Thioacetyl Cation (2^+), and Isothioacetyl Cation (3^+). Similar to its parent radical HCS,[31] **2** has a bent structure. It is the second lowest energy $[C_2H_3S]$ isomer. It is 36 kJ mol^{-1} higher in energy than **1**. The methyl group in **2** essentially rotates freely. The rotational TS **2a** is 2 kJ mol^{-1} higher in energy than **2**. Radical **3**, the iso form of **2**, also has a bent C−C−S skeleton, as in HSC. The latter is 164 kJ mol^{-1} higher in energy than HCS.[31] Radical **3** is 177 kJ mol^{-1} higher in energy than **2** and its rotational TS (**3a**) is only 1 kJ mol^{-1} higher in energy than **3**.

Removal of the unpaired electron localized on the thiocarbonyl carbon yields $\mathbf{2}^+$ which has a linear C−C−S skeleton. It is the lowest energy isomer of $[C_2H_3S]^+$ ions found in this work as well as in other studies.[6] The calculated ΔH_{f298} of $\mathbf{2}^+$ is 885 kJ mol^{-1}, in good agreement with Caserio and Kim's estimated value (879 kJ mol^{-1}),[4] but not with the value (854 kJ mol^{-1}) compiled by Lias et al.[12] We have discussed the reliability of the compiled ΔH_{f298} value for $\mathbf{2}^+$ in our recent report.[18] Cation $\mathbf{3}^+$, derived from **3** upon ionization, has a cyclic-like structure and is higher in energy than $\mathbf{2}^+$ by 339 kJ mol^{-1}. The parent cation, HSC^+, has bridged structure and is 317 kJ mol^{-1} higher in energy than the linear HCS^+ at the G2 level.[32]

A NBO analysis reveals that $\mathbf{3}^+$ has a three-centered bond involving the three non-hydrogen atoms and the CS moiety carries most of the charge (0.74 e). These results, together with the structural parameters of $\mathbf{3}^+$ as shown in Figure 3, suggest that it is a $\sigma-\pi$ complex consisting of CH_3^+ and CS fragments. The methyl group rotates quite freely about the S−CH_3 bond. The rotational TS ($\mathbf{3a}^+$) is 8 kJ mol^{-1} higher in energy than $\mathbf{3}^+$.

3.1.3. Cyclic $[C_2H_3S]$ Radicals (4, 5, 6, 7) and $[C_2H_3S]^+$ Ions (4^+, 5^+, 7^+). The cyclic radical **4** has C_1 symmetry and is the third lowest energy isomer on the $[C_2H_3S]$ PES. Energetically, it is 87 kJ mol^{-1} above **1**. The S−CH_2 bond (1.853 Å) is longer than the S−CH bond (1.742 Å). The inversion barrier for **4** at the radical center is small, about 9 kJ mol^{-1}. The inversion TS (**4a**) has C_s symmetry.

Two conformers of the cyclic thiirenium radical, **5** and **6**, were located at the UQCISD/6-31G(d) level. While **5** with C_s symmetry has its S−H bond trans to both C−H bonds, the asymmetric conformer **6** has its C−H bonds trans to each other. The latter is slightly lower in energy than the former by 2 kJ mol^{-1} and is 282 kJ mol^{-1} higher in energy than **1**. Results of a NBO analysis indicate that the C−C bond is due to a three-electron two-center (3e−2c) interaction[33−37] and the two C

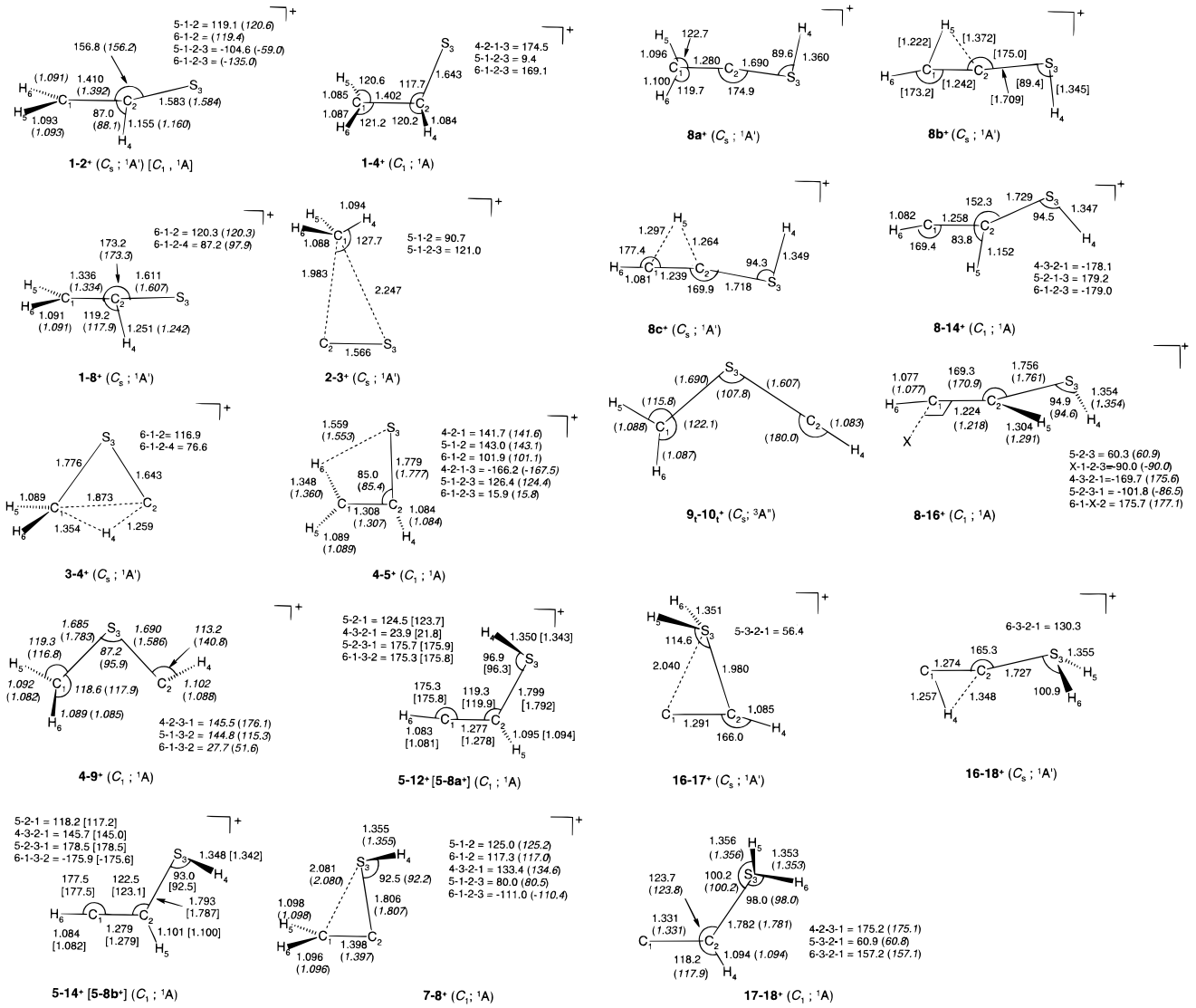

Figure 4. Transition-state structures for $[C_2H_3S]^+$ ions optimized at the RQCISD/6-31G(d), UQCISD/6-31G(d) (italic numbers in parentheses), RCCSD/6-31G(d) (italic numbers) and RQCISD/6-311G(d,p) (numbers in square brackets) levels. TSs **5**−**12**$^+$ and **5**−**14**$^+$ becomes **5**−**8a**$^+$ and **5**−**8b**$^+$, respectively, at the RQCISD/6-311G(d,p) level. Structural parameters for **1**−**4**$^+$ are based on RCISD/6-31G(d) optimization.

atoms carry most of the α-spin density (about 0.5 at each site). These features are also reflected by the unusual structure of **5/6**: the carbonic centers are pyramidal and the C−C bond (1.37 Å for **5** and 1.39 Å for **6**) has partial double bond character. Conversion of **5** to **6** involves inversion at one of the C atoms. The inversion TS **5**−**6** is 18 kJ mol^{-1} higher in energy than **5**. The cyclic structure (**14**−**14**) with all three H atoms on the same side does not correspond to a local minimum on the UQCISD/6-31G(d) PES but a TS structure via which **14** converts to itself on ring closing and opening. It has the same energy as **5**.

For **7**, the unpaired p electron is mainly localized on the unsubstituted carbon. The C−SH single bond is unusually long (2.079 Å), as compared to the H_2C−SH bond which is 1.847 Å. Among the cyclic isomers, this has the highest energy, 297 kJ mol^{-1} above **1**.

On ionization of **4**, **5/6**, and **7**, thiiranyl (**4**$^+$) and thiirenium (**5**$^+$) cations, and a cyclic carbenoid species (**7**$^+$) are formed, respectively. The thiiranyl ion is the third lowest energy isomer among the $[C_2H_3S]^+$ ions studied in this work and is 116 kJ mol^{-1} higher in energy than **2**$^+$. The positive charge is mainly localized on the S atom, suggesting the resonance structure *c*-CH_2SC^+H (a cyclic carbenium ion) is insignificant. The S−CH bond (1.609 Å) is atypical of a C−S double bond (1.62 Å). Thiirenium ion (**5**$^+$) is 33 kJ mol^{-1} higher in energy than **4**$^+$. Its structure is quite similar to its radical precursor **5**. The carbenoid cation **7**$^+$, which has not been studied before, is 253 kJ mol^{-1} higher in energy than **4**$^+$. The bonds within the rings of the cyclic cations are shorter than those calculated for the corresponding radical precusors, consistent with a tightening of bonds resulting from the positive charge on the ring.[38,39]

3.1.4. 1-Thiovinyl Radical (8) and Cation (8$^+$*).* Radical **8** has C_1 symmetry with the S−H bond trans to the CH_2 group. It is ca. 100 kJ mol^{-1} higher in energy than **1**. Rotation about the C−S bond proceeds without a barrier. The rotational TSs **8a** and **8b** are ca. 8 and 13 kJ mol^{-1}, respectively, above **8**.

The conformation of **8**$^+$, which has C_s symmetry, is very different from that of **8**. Both the C−C and C−S bonds of **8**$^+$ have double bond character and its valence structure is isoelectronic with allene (CH_2CCH_2). On protonation at the S atom of thioketene, which has C_{2v} symmetry, the H_2C−C−S moiety only slightly deviates from planarity with the S−H bond approximately orthogonal to its molecular plane. Cation **8**$^+$ is higher in energy than **2**$^+$ by 106 kJ mol^{-1} and is the second lowest energy cation among the $[C_2H_3S]^+$ isomers. The rotational TS (**8a**$^+$) is 127 kJ mol^{-1} above **8**$^+$. Its transition vector has major out-of-plane components involving the me-

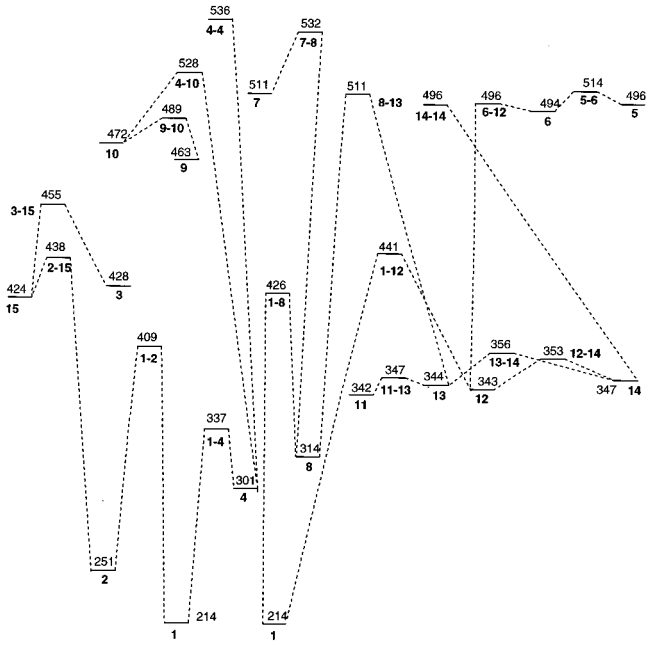

Figure 5. $G2_{UQCISD}$ potential energy surface for $[C_2H_3S]$ radicals. Energies (ΔH_{f0}, kJ mol^{-1}) are not drawn to scale.

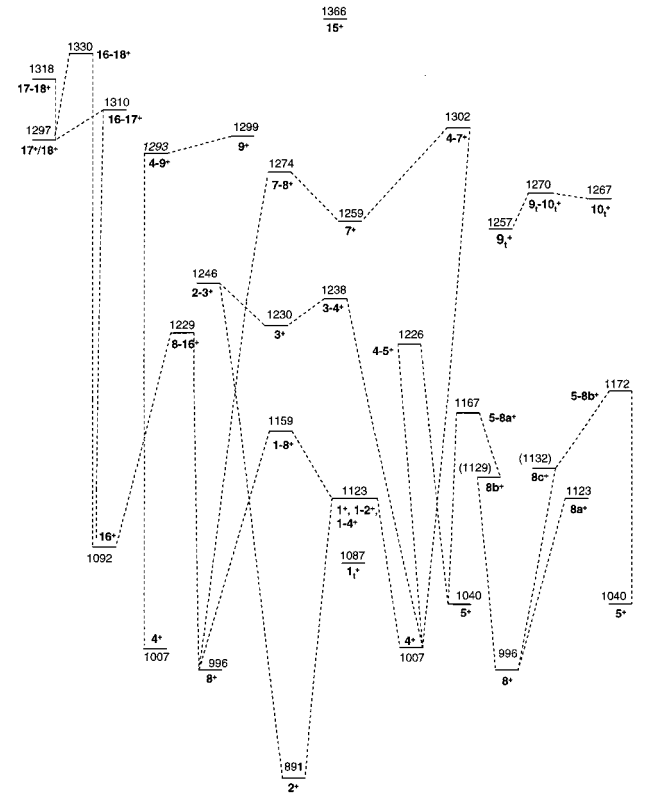

Figure 6. $G2_{RQCISD}$ potential energy surface for $[C_2H_3S]^+$ ions. Energies (ΔH_{f0}, kJ mol^{-1}) are not drawn to scale. Numbers in parentheses are $G2_{RQCISD}$ ΔH_{f0} values based on RQCISD/6-311G(d,p) structures and frequencies.

thylenic and thiol H atoms. This indicates that rotation of the S−H bond about the C−S bond is accompanied by the rotation of the CH_2 group about the C−C bond or vice versa. Two nonclassical TSs (**8b**$^+$ and **8c**$^+$) having structural features similar to the nonclassical vinyl cation[16] were located. The former could not be identified at the RQCISD/6-31G(d) level but could be found at the RMP2/6-311G(d,p) and RQCISD/6-311G(d,p) levels. Because of the larger basis set used, it was characterized by IRC calculations at the RMP2/6-311G(d,p) level. They are 132 and 138 kJ mol^{-1} higher in energy than **8**$^+$, respectively. They lead to no other isomeric $[C_2H_3S]^+$ ions but **8**$^+$. Their transition vectors have major out-of-plane components associated with all the H atoms. They can be considered as rotational TSs involving *incomplete* 1,2-H shift of **8**$^+$.

*3.1.5. CH_2SCH (**9**/**10**) and CH_2S^+CH (**9**$^+$, **9**$_t^+$/**10**$_t^+$).* Two conformers, trans (**9**) and cis (**10**), of CH_2SCH with C_s symmetry were found. Their zeroth-order UHF/6-31G(d) wave functions suffer from spatial symmetry-breaking.[40−42] Nevertheless, the calculated energies of the C_1 structures (based on C_1 UHF-stable wave functions) are essentially the same as those of the corresponding C_s structures (based on UHF-unstable wave functions). It is also well-known that unstable wave functions may have dramatic effects on the calculation of vibrational frequencies.[43,44] In the present cases, the computed frequencies for the C_s structures agree with (within 8 cm^{-1}) those for the C_1 structures.

The trans isomer is 249 kJ mol^{-1} higher in energy than **1** and is ca. 9 kJ mol^{-1} lower in energy than the cis conformer. The ΔE_b for **9** → **10** is 26 kJ mol^{-1}. The TS **9**−**10** was calculated by using the UHF-unstable function as the zeroth-order reference wave function.

Cation **9**$_t^+$/**10**$_t^+$, which has not been discussed before, can be considered as a substituted methylene. The cis conformer, **10**$_t^+$ (^{3}A″) is higher in energy than **9**$_t^+$ (^{3}A″) by 10 kJ mol^{-1}. Both S−CH_2 and S−CH bonds of **9**$_t^+$/**10**$_t^+$ have double bond character: three π electrons delocalize among the three heavy atoms. Conversion of **9**$_t^+$ into **10**$_t^+$ may proceed via the inversion TS (**9**$_t$−**10**$_t^+$) and has a ΔE_b of 13 kJ mol^{-1}. The closed-shell structure, **9**$^+$ (**1**A′), suffers from RHF-unstable wave functions, as in the cases of **1**$^+$, CH_2, and O_2. It can be considered as an open form of **4**$^+$ and is ca. 42 kJ mol^{-1} above **9**$_t^+$. This ΔE_{ST} is similar to that for **1**$^+$. As will be discussed later, it readily collapses to **2**$^+$ or **4**$^+$.

*3.1.6. 2-Thiovinyl Radical (**11**/**12**/**13**/**14**) and Cation (**12**$^+$/**14**$^+$).* As shown in Figure 2, there are four conformers (**11**, **12**, **13**, and **14**) for the 2-thiovinyl radical. All of these conformers have essentially the same energy (Table 1). Among them, **11** has the lowest energy and **14** has the highest energy. They are ca. 101−105 kJ mol^{-1} higher in energy than **1**. The rotational TSs **13a** and **14a** have about the same energy as **13** and **14**, respectively. Conformer **11** can isomerize to **12** and **13** via TSs **11**−**12** and **11**−**13**, respectively. Conversions of **14** to **12** and **13** may proceed via TSs **12**−**14** and **13**−**14**, respectively. The ΔE_bs for these rearrangements are small, no more than 12 kJ mol^{-1}. In summary, the 2-thiovinyl radical is highly flexible and adopts a wide range of conformations.

Two conformers of the 2-thiovinyl cation were found at the RQCISD/6-31G(d) level. The anti conformer (**14**$^+$) is slightly lower in energy than the syn conformer (**12**$^+$) by 6 kJ mol^{-1} and is ca. 269 kJ mol^{-1} above **2**$^+$. The zeroth-order RHF wave function of **12**$^+$ is slightly unstable to symmetry breaking.[40−42] However, both do not correspond to local minima and collapse to **8**$^+$ at the RMP2/6-311G(d,p) and RQCISD/6-311G(d,p) levels.

*3.1.7. S-Protonated Ethynylthiol (**16**$^+$) and Thiovinylidene (**17**$^+$, **18**$^+$).* Cation **16**$^+$ has a C_s structure at the RQCISD/6-31G(d) level. It is 202 kJ mol^{-1} higher in energy than **2**$^+$. Previous HF calculations[6] indicate that **16**$^+$ has a C_{2v} structure and is 361 kJ mol^{-1} higher in energy than **2**$^+$.

S-Protonated thiovinylidene belongs to a class of unsaturated carbenes[45] which have attracted a great deal of attention in organic chemistry.[45−48] The simplest unsaturated carbene is

vinylidene[45] ($H_2C{=}C{:}$) whose existence has been the subject of experimental and computational studies.[49] The two conformers of S-protonated thiovinylidene, $\mathbf{17}^+$ and $\mathbf{18}^+$, have similar energy ($\Delta H_{f0} = 1297$ kJ mol^{-1}). Interconversion between them occurs via the rotational TS $\mathbf{17}-\mathbf{18}^+$ which lies ca. 21 kJ mol^{-1} above $\mathbf{17}^+/\mathbf{18}^+$. The energy barrier for the inversion at the S atom of $\mathbf{17}^+/\mathbf{18}^+$ is expected to be similar to that (110 kJ mol^{-1}) for the protonated vinyl thiol cation.[15]

3.2. Isomerizations of $[C_2H_3S]$. *3.2.1. Intramolecular Rearrangements of* ***1****.* Four radicals (**2**, **4**, **8**, and **12**) can be derived from **1**. The 1,2-H shifts **1** → **2** and **1** → **8** proceed via TSs **1**−**2** and **1**−**8**, respectively. Their respective ΔE_bs are 195 and 212 kJ mol^{-1}. The corresponding reverse barriers are 159 and 112 kJ mol^{-1}. Radical **1** can be considered as the open form of **4**. The TS **1**−**4** for **1** → **4** is 123 kJ mol^{-1} above **1**. The low-energy barrier for the reverse process, as discussed in section 3.2.3, may pose difficulty in the experimental observation of **4**.

Formation of **12** from **1** can be achieved through 1,3-H shift. Examining TS **1**−**12**, one may contend that the process is in fact an internal H abstraction. It lies 227 and 98 kJ mol^{-1} above **1** and **12**, respectively.

3.2.2. Interconversion between ***2*** *and* ***3****.* We found no TS (for 1,2-methyl shift) connecting **2** and **3** on the UQCISD/6-31G(d) PES. Nevertheless, interconversion between **2** and **3** may be achieved through a dissociation/recombination mechanism: **2** → CS + CH_3 (**15**) → **3**. The barrier height for **2** → **15** is 188 kJ mol^{-1} and that for **3** → **15** is substantially lower, 27 kJ mol^{-1}. The latter value is even smaller (6 kJ mol^{-1}) after SCC. It is thus anticipated that observation of **3** will be difficult as it decomposes readily. The TSs **2**−**15** and **3**−**15** are 14 and 31 kJ mol^{-1} above **15**, respectively.

*3.2.3. Intramolecular Rearrangements of the Cyclic Isomers (****4****,* ***5/6****, and* ***7****) and Thiovinyl Radicals (****8****,* ***11/12/13/14****).* Ring opening and concomitant rotation of the CH_2 group of **4** lead to the formation of **1** via **1**−**4** which is 36 kJ mol^{-1} above **4**. Since the UHF function of **1**−**4** is seriously spin-contaminated ($\langle S^2\rangle \approx 1.06$), the ΔE_b may be as low as 10 kJ mol^{-1} after SCC. Observation of **4** may be difficult due to its readiness to convert to **1**. Hydrogen scrambling between the two carbons may also occur via 1,2-H shift. However, this is a high-energy process with a barrier of 235 kJ mol^{-1}. The TS **4**−**4** has C_s symmetry. Another open form of **4** is **10** which can be formed by breaking the C−C bond of **4**. This ring-opening reaction is also a high-energy process with a barrier of 227 kJ mol^{-1}. The UHF wave function for **4**−**10** is unstable. Its UHF-stable reference wave function has a heavy mix with a higher-energy quintet state and is thus seriously spin-contaminated ($\langle S^2\rangle \approx 1.67$). With this reference wave function as initial guess, the calculated ΔE_b is 250 kJ mol^{-1}. This value decreases to 225 kJ mol^{-1} with SCC, close to the value (227 kJ mol^{-1}) calculated with the UHF-unstable function which has $\langle S^2\rangle \approx 0.79$. The reverse ΔE_b is 56 kJ mol^{-1}. The $PG2_{UQCISD}$ value is 61 kJ mol^{-1}.

The open form of **5/6** is **11/12**. The ΔE_b for **6** → **12** is essentially zero at the $G2_{UQCISD}$ level, suggesting that **5/6** readily collapses to **12**. In addition, the structure of TS **6**−**12** is very similar to that of **6**. Thus, one may regard that **5** → **12** essentially proceeds via a TS having a spectrum of structures of **5**−**6**, **6**, and **6**−**12** with a ΔE_b (18 kJ mol^{-1}) similar to that for **5** → **6**. Because of their high energies and readiness to collpase to **12**, both **5** and **6** are chemically insignificant.

Radical **7**, like **5**/**6**, is also relatively unimportant since it is quite high in energy and the barrier to collapse to its open form (**8**) is rather small, 21 kJ mol^{-1}. The TS **7**−**8** is intermediate between **7** and **8**. The latter may rearrange to **13** via TS **8**−**13**. This 1,2-H shift has a barrier of 198 kJ mol^{-1}. As can be seen from Table 1, **8** is slightly lower in energy than the 2-thiovinyl radical (**11/12/13/14**) by ca. 28 kJ mol^{-1}. Among the rearrangements **8** → **1**, **8** → **7**, and **8** → **13**, the first one (with a ΔE_b of 112 kJ mol^{-1}) is the most competitive from an energetic viewpoint.

3.3. Intramolecular Rearrangements of $[C_2H_3S]^+$. Common to all the experiments, CAD and surface-induced dissociation (SID), investigated by Cooks et al.[3] is the finding that different $[C_2H_3S]^+$ ions derived from different precursors yield very similar spectra. The available data[3] suggest that the originally formed $[C_2H_3S]^+$ species have reached a common structure or mixture of structures prior to fragmentation. Cations $\mathbf{1}^+$, $\mathbf{2}^+$, $\mathbf{4}^+$, $\mathbf{5}^+$, $\mathbf{8}^+$, and ($\mathbf{12}^+/\mathbf{14}^+$) were deduced as plausible structural possibilities.[3] In particular, SID and low-energy CAD spectra are remarkably similar.[3] Their main feature is the presence of a dominant peak at *m*/*z* 15 in contrast to the high-energy CAD spectra which virtually have no peak at *m*/*z* 15.[3,5] The presence of a prominent peak at *m*/*z* 15 in SID and low-energy CAD spectra strongly suggests that at least one of the common structures is $\mathbf{2}^+$. The barrier for $\mathbf{2}^+ \rightarrow CH_3^+ + CS$ ($\mathbf{15}^+$) is 474 kJ mol^{-1}. This threshold is well above most of the barriers (Figure 6) for the intramolecular rearrangements of the $[C_2H_3S]^+$ ions. It was proposed that the virtual absence of the peak at *m*/*z* 15 in high-energy CAD experiments is due to fragmentation via an excited electronic state in those CAD experiments that proceed via electronic excitation.[3] Translational energy spectroscopy has also been used to study the electronic transitions between the low-lying nondissociative electronic states of $\mathbf{2}^+$.[2]

3.3.1. Isomerizations of $\mathbf{4}^+$*. (a)* $\mathbf{4}^+ \rightarrow \mathbf{2}^+$**.** On the QCISD/6-31G(d) PES, it appears that conversion of $\mathbf{4}^+$ to $\mathbf{2}^+$ may proceed via two pathways which involve intermediates $\mathbf{1}^+$ and $\mathbf{3}^+$, respectively. The lower-energy pathway $\mathbf{4}^+ \rightarrow \mathbf{1}^+ \rightarrow \mathbf{2}^+$ has a ΔE_b of ca. 116 kJ mol^{-1} (Figure 6). At the $G2_{RQCISD}$ level, $\mathbf{1}^+$ lies 12 and 127 kJ mol^{-1} above TS $\mathbf{1}-\mathbf{2}^+$ and $\mathbf{4}^+$ (Table 2), respectively. The anomaly that a TS is slightly lower in energy than a local minimum to which it connects has been discussed previously.[50] In addition, in regions of the PES having a triplet ground state (the ground state of $\mathbf{1}^+$ is a spin triplet), the RHF function of the system is unstable[19] and the accuracy of restricted Møller−Plesset energies based on RHF-unstable functions is questionable.[51] Also, such a *problematic* system may suffer from unsatisfactory convergence of unrestricted Møller−Plesset perturbation energies.[52,53] We failed to locate TS $\mathbf{1}-\mathbf{4}^+$ at the RQCISD/6-31G(d) level. However, at the $G2_{RCISD}$ level, $\mathbf{1}^+$ is about 3 kJ mol^{-1} above $\mathbf{1}-\mathbf{4}^+$. From Figure 4, one may notice that the structure of $\mathbf{1}-\mathbf{4}^+$ is very slightly distorted from that of $\mathbf{1}^+$. While the difference between the $G2_{RQCISD}$ and $G2_{RCISD}$ electronic energies of $\mathbf{1}^+$ is small (ca. 3 kJ mol^{-1}), the scaled ZPE obtained at the RQCISD/6-31G(d) level is significantly larger (by 11 kJ mol^{-1}) than that calculated at the RCISD/6-31G(d) level. This large difference may be due to the zeroth-order RHF-unstable function of $\mathbf{1}^+$, which may have dramatic effects on the calculation of vibrational frequencies.[43,44] In fact, $\mathbf{1}^+$ is a first-order saddle point at the RMP2/6-31G(d) and RCCSD/6-31G(d) levels. The $G2_{RCCSD}$ $\Delta H_{f0}(\mathbf{1}^+)$, 1119 kJ mol^{-1}, is close to the $G2_{RCISD}$ ΔH_{f0} ($\mathbf{1}-\mathbf{4}^+$) value, 1123 kJ mol^{-1}. In the environs of TS $\mathbf{1}-\mathbf{2}^+$, the singlet state becomes lower in energy than the triplet state. Nevertheless, its RHF function is still unstable with respect to UHF conversion. Its $G2_{UQCISD}$ energy is ca. 38 kJ mol^{-1} larger than its $G2_{RQCISD}$ value due to higher spin contamination. As can be seen from Table 2, the calculated $PG2_{UQCISD}$ ΔH_{f0} (1119 kJ mol^{-1}) of

$\mathbf{1}-\mathbf{2}^+$ is very close to its $G2_{RQCISD}$ ΔH_{f0} value (1122 kJ mol^{-1}). The overall picture of these results is that the PES in the environs of $\mathbf{1}^+$ is very flat. Conformer $\mathbf{1}^+$ may be in fact a TS structure for the ring opening−closing process $\mathbf{4}^+ \rightarrow \mathbf{4}^+$, which in turn connects to TSs $\mathbf{1}-\mathbf{2}^+$ and $\mathbf{1}-\mathbf{8}^+$. It seems that the structure $\mathbf{1}-\mathbf{4}^+$ obtained at the RCISD/6-31G(d) level is an artifact due to the problems[18,41,42,49] arising from an RHF-unstable wave function. The ring-opening process $\mathbf{4}^+ \rightarrow \mathbf{1}^+$ may feature crossing with any triplet PES in the vicinity of the minimum energy path close to $\mathbf{1}^+$, resulting in the formation of $\mathbf{1}_t^+$. In the subsequent discussion, we consider $\mathbf{1}^+$ as a TS and its $G2_{RCCSD}$ energy is used for energetics comparison. In summary, one may consider the rearrangement $\mathbf{4}^+ \rightarrow \mathbf{2}^+$ proceeds via a TS with a spectrum of structures ($\mathbf{1}^+$and $\mathbf{1}-\mathbf{2}^+$) and has a ΔE_b of ca. 116 kJ mol^{-1}. The reverse ΔE_b, 232 kJ mol^{-1}, is still far less than the enthalpy of reaction ΔH_{r0} (475 kJ mol^{-1}) for the dissociation $\mathbf{2}^+ \rightarrow \mathbf{15}^+$.

An alternative pathway for $\mathbf{4}^+ \rightarrow \mathbf{2}^+$ is via intermediate $\mathbf{3}^+$ as well as TSs $\mathbf{3}-\mathbf{4}^+$ and $\mathbf{2}-\mathbf{3}^+$ (Figure 6). The overall ΔE_b is 240 kJ mol^{-1}. Energetically, this pathway is less competitive than the one proceeding via the open structure $\mathbf{1}^+$.

(b) $\boldsymbol{4}^+ \rightarrow \boldsymbol{5}^+$. Through 1,2-H shift, $\mathbf{4}^+$ rearranges to $\mathbf{5}^+$ with a barrier of 219 kJ mol^{-1}. The TS $\mathbf{4}-\mathbf{5}^+$ resembles a four-membered ring structure and is 186 kJ mol^{-1} above $\mathbf{5}^+$.

(c) $\boldsymbol{4}^+ \rightarrow \boldsymbol{8}^+$. Conversion of $\mathbf{4}^+$ to $\mathbf{8}^+$ may proceed via TSs $\mathbf{1}^+$ and $\mathbf{1}-\mathbf{8}^+$ or the cyclic carbenoid intermediate $\mathbf{7}^+$. From Figure 6, it may be concluded that the former pathway is more energetically competitive and its overall ΔE_b is 152 kJ mol^{-1}. The limiting step of the latter pathway has a barrier of 296 kJ mol^{-1}. Ring opening of $\mathbf{7}^+$ leads to the formation of $\mathbf{8}^+$ via $\mathbf{7}-\mathbf{8}^+$ and is a facile process with a barrier of 14 kJ mol^{-1}.

(d) $\boldsymbol{4}^+ \rightarrow \boldsymbol{9}^+$. On the singlet PES, $\mathbf{9}^+$ would be formed upon cleavage of the C−C bond of $\mathbf{4}^+$ with a barrier of ca. 287 kJ mol^{-1}. Since, $\mathbf{9}_t^+$ is lower in energy, the scenario of the PES in the vicinity of $\mathbf{9}^+$ would be similar to that of $\mathbf{1}^+$ as mentioned above. We successfully located TS $\mathbf{4}-\mathbf{9}^+$ at the RCISD/6-31G(d) and RCCSD/6-31G(d) levels, but not at the RQCISD/6-31G(d) level. The IRC calculations for $\mathbf{4}-\mathbf{9}^+$ were carried out at the former theoretical level. The $G2_{RCISD}$ ΔH_{f0} (1292 kJ mol^{-1}) and the $G2_{RCCSD}$ ΔH_{f0} (1293 kJ mol^{-1}) for $\mathbf{4}-\mathbf{9}^+$ are ca. 6 kJ mol^{-1} less than the $G2_{RQCISD}$ ΔH_{f0} ($\mathbf{9}^+$). If $\mathbf{9}^+$ corresponds to a local minimum, it would then be a very shallow one and readily collapse to $\mathbf{4}^+$. Formation of $\mathbf{9}_t^+/\mathbf{10}_t^+$ may result from intersystem crossing in the vicinity of the minimum energy paths of the ring opening processes close to $\mathbf{9}^+$.

3.3.2. Rearrangement $\boldsymbol{5}^+ \rightarrow \boldsymbol{8}^+$. We found $\mathbf{5}^+$ may rearrange to $\mathbf{8}^+$ via intermediate $\mathbf{14}^+$ and TSs $\mathbf{5}-\mathbf{14}^+$ and $\mathbf{8}-\mathbf{14}^+$ at the RQCISD/6-31G(d) level. Previous HF results[6] also predict that heterolysis of one of the C−S bonds of $\mathbf{5}^+$ would lead to the formation of $\mathbf{12}^+/\mathbf{14}^+$. The HF calculated TS structures ($\mathbf{5}-\mathbf{12}^+$ and $\mathbf{5}-\mathbf{14}^+$) are 5−11 kJ mol^{-1} above the latter,[6] in good agreement with the $G2_{RQCISD}$ results (2−13 kJ mol^{-1}). Though $\mathbf{14}^+$ corresponds to a local minimum at the RQCISD/6-31G(d) level, its $G2_{RQCISD}$ energy is 13 kJ mol^{-1} higher than that of $\mathbf{8}-\mathbf{14}^+$, suggesting that the former may not actually be at a minimum.

Since $\mathbf{12}^+$ and $\mathbf{14}^+$ collapse to $\mathbf{8}^+$ at both the RMP2/6-311G(d,p) and RQCISD/6-311G(d,p) levels, one may suspect that the RQCISD/6-31G(d) structures $\mathbf{5}-\mathbf{12}^+$ and $\mathbf{5}-\mathbf{14}^+$ would become TSs $\mathbf{5}-\mathbf{8a}^+$ and $\mathbf{5}-\mathbf{8b}^+$, respectively, which connect $\mathbf{5}^+$ and $\mathbf{8}^+$ at the RMP2/6-311G(d,p) or RQCISD/6-311G(d,p) level. The IRC calculations for $\mathbf{5}-\mathbf{8a}^+$ and $\mathbf{5}-\mathbf{8b}^+$ were performed at the RMP2/6-311G(d,p) level. In addition, along these IRC paths, structures similar to $\mathbf{8b}^+$ and $\mathbf{8c}^+$ are involved. In summary, isomerization $\mathbf{5}^+ \rightarrow \mathbf{8}^+$ may proceed via TS $\mathbf{5}-\mathbf{8a}^+$ (ΔE_b = 127 kJ mol^{-1}) or TS $\mathbf{5}-\mathbf{8b}^+$ (ΔE_b = 133 kJ mol^{-1}).

3.3.3. Formation of S-Protonated Ethynylthiol ($\boldsymbol{16}^+$*) and S-Protonated Thiovinylidene (*$\boldsymbol{17}^+/\boldsymbol{18}^+$*).* The H_2S group is a common feature to cations $\mathbf{16}^+$ and $\mathbf{17}^+/\mathbf{18}^+$. High-energy CAD and angle-resolved spectra of $[C_2H_3S]^+$ ions generated from precursors containing no HS or H_2S moiety show a small peak at *m*/*z* 34 (H_2S^+).[3,5] It is not unreasonable to assume that in most cases, $[C_2H_3S]^+$ ions formed in the ion source initially have the skeletal features of their neutral precursors. Thus, a simple explanation for the appearance of the peak at *m*/*z* 34 in these CAD spectra is that a small portion of initially generated $[C_2H_3S]^+$ ions which contain no H_2S group has undergone rearrangement to $[C_2H_3S]^+$ ions containing the H_2S group prior to fragmentation. On the other hand, low-energy CAD spectra of $[C_2H_3S]^+$ ions show no intensity at *m*/*z* 34.[3]

In term of thermochemical stability, $\mathbf{16}^+$ (ΔH_{f0} = 1093 kJ mol^{-1}) is comparable to $\mathbf{5}^+$ (ΔH_{f0} = 1040 kJ mol^{-1}). The carbenoid species, $\mathbf{17}^+/\mathbf{18}^+$, are considerable higher in energy ($\Delta H_{f0}(\mathbf{17}^+/\mathbf{18}^+)$ = 1297 kJ mol^{-1}) than $\mathbf{2}^+$, $\mathbf{4}^+$, $\mathbf{5}^+$, and $\mathbf{16}^+$. In addition, the ΔE_bs for the formation of $\mathbf{17}^+/\mathbf{18}^+$ from $\mathbf{16}^+$ are relatively large (e.g., 217 kJ mol^{-1} for 1,2-H shift $\mathbf{16}^+ \rightarrow \mathbf{17}^+$ via $\mathbf{16}-\mathbf{17}^+$ and 237 kJ mol^{-1} for 1,2-H_2S shift $\mathbf{16}^+ \rightarrow \mathbf{18}^+$ via $\mathbf{16}-\mathbf{18}^+$). Consequently, $\mathbf{17}^+/\mathbf{18}^+$ would not be a plausible candidate responsible for the peak at *m*/*z* 34. Ion $\mathbf{16}^+$ can be formed from $\mathbf{8}^+$ via TS $\mathbf{8}-\mathbf{16}^+$ with a ΔE_b of 232 kJ mol^{-1}. This 1,3-H shift is considerably less competitive compared to other rearrangements of $\mathbf{8}^+$: $\mathbf{8}^+ \rightarrow \mathbf{2}^+/\mathbf{4}^+$ via $\mathbf{1}^+$ (ΔE_b = 162 kJ mol^{-1}) and $\mathbf{8}^+ \rightarrow \mathbf{5}^+$ via $\mathbf{5}-\mathbf{8a}^+/\mathbf{5}-\mathbf{8b}^+$ ($\Delta E_b \approx$ 175 kJ mol^{-1}). Thus, under the condition of low-energy collision, virtually no $\mathbf{16}^+$ would be formed. Even if a significant amount of $\mathbf{16}^+$ could be formed from $\mathbf{8}^+$, it would have reverted back to $\mathbf{8}^+$ prior to fragmentation since the ΔE_b for $\mathbf{16}^+ \rightarrow \mathbf{8}^+$ is 137 kJ mol^{-1} and the ΔH_{r0} (considered as the lower bound of ΔE_b) for the dissociation $\mathbf{16}^+ \rightarrow H_2S^+ + HCC$ is 468 kJ mol^{-1}. High-energy angle-resolved CAD experiments impart a certain amount of internal energy into the parent ion, which increases with scattering angle.[3] Angle-resolved spectra for $[C_2H_3S]^+$ ions show that at larger scattering angles, ionic fragments (*m*/*z* 44, 32, 26) which are expected to have high energies of activation increase in abundance.[3] We noticed that these spectra also show the same trend for the ionic fragment *m*/*z* 34, suggesting the energy of activation for $[C_2H_3S]^+ \rightarrow H_2S^+ + HCC$ is high. The calculated ΔH_{r0}, the lower bound of ΔE_b, for $\mathbf{16}^+ \rightarrow H_2S^+ + HCC$ is in line with observation.

It is worthwhile mentioning that Chase's compiled ΔH_{f298}(HCC),[54] 477 kJ mol^{-1}, is ca. 100 kJ mol^{-1} smaller than the $G2_{UQCISD}$ ΔH_{f298}(HCC) value (577 kJ mol^{-1}). This difference becomes smaller (59 kJ mol^{-1}) after SCC. On the other hand, Tsang's[55] reported ΔH_{f298}(HCC) value, 556 ± 8 kJ mol^{-1}, is between our $G2_{UQCISD}$ and $PG2_{UQCISD}$ ΔH_{f298}(HCC) values. Our calculated ionization energy (11.7 eV) for HCC is in good agreement with the evaluated value (11.61 ± 0.07 eV) listed in ref 13. The calculated electron affinity (3.06 eV) for HCC is also in agreement with the more recent experimental data (2.92−2.98 eV).[56−58] In addition, the $G2_{UQCISD}$ proton affinity (773 kJ mol^{-1}) at 298 K for HCC is in fair agreement with the value (753 kJ mol^{-1}) evaluated by Hunter and Lias.[59]

4. Conclusion

Ten $[C_2H_3S]$ isomers have been identified. Thioformylmethyl radical (**1**) has the lowest energy and its ΔH_{f0} is 214 kJ mol^{-1}. The next three lowest energy isomers are **2**, **4**, and **8,** as illustrated in Figure 5. Radical 1-thiolvinyl (**8**) is found to be 28−33 kJ mol^{-1} lower in energy than the 2-thiovinyl radical

(**11**/**12**/**13**/**14**) which may adopt a wide spectrum of conformations because of the flexibility of the radical. Isomerizations of **2**, **4**, **8**, and **12** lead to the formation of **1**. Their ΔE_bs range from 36 to 158 kJ mol^{-1}. Formation of **3** from **2** proceeds via a dissociation and recombination mechanism: **2** → **15** → **3**. The dissociation stage has energy barrier of 187 kJ mol^{-1}, and the recombination step has a small ΔE_b (31 kJ mol^{-1}). Other radicals (**5**/**6**, **7**, **8**, **9**/**10**) are high-energy species with ΔH_{f0} values larger than 460 kJ mol^{-1}.

The ground state of thioformylmethyl cation is a spin triplet ($\mathbf{1}_t^+$), not a closed-shell singlet ($\mathbf{1}^+$). The singlet structure corresponds to a local minimum at the RQCISD/6-31G(d) level but a TS at the RCCSD/6-31G(d) level. In view of the flatness of the PES in the environs of $\mathbf{1}^+$ (Figure 6), whether it is a local minimum or a TS structure makes no difference under CAD experimental conditions. Nevertheless, it is an important open structure involved in conversions among $\mathbf{2}^+$, $\mathbf{4}^+$, and $\mathbf{8}^+$. Among the $[C_2H_3S]^+$ ions, $\mathbf{2}^+$ with a ΔH_{f0} value of 891 kJ mol^{-1} has the lowest energy. We have commented[18] on the accuracy of the compiled $\Delta H_{f298}(\mathbf{2}^+)$ value (854 kJ mol^{-1}) of Lias et al.[12] Among the three cyclic $[C_2H_3S]^+$ ions ($\mathbf{4}^+$, $\mathbf{5}^+$, and $\mathbf{7}^+$), the carbenoid species $\mathbf{7}^+$ has the highest energy. The carbenoid species $\mathbf{9}_t^+$/$\mathbf{10}_t^+$ is high in energy. Ring openings of $\mathbf{4}^+$ may lead to open singlet species $\mathbf{1}^+$ and $\mathbf{9}^+$ which are not ground states. These processes may feature intersystem crossings in the vicinity of the minimum energy paths close to $\mathbf{1}^+$ and $\mathbf{9}^+$, resulting in the formation of $\mathbf{1}_t^+$ and $\mathbf{9}_t^+$/$\mathbf{10}_t^+$, respectively. Both $\mathbf{1}^+$ and $\mathbf{9}^+$ may actually be TSs for the ring-opening processes of $\mathbf{4}^+$, although they correspond to shallow minima at the RQCISD/6-31G(d) level.

Cations $\mathbf{2}^+$, $\mathbf{5}^+$, and $\mathbf{8}^+$ can be obtained from isomerizations of $\mathbf{4}^+$. The barriers for these rearrangements range from 116 to 220 kJ mol^{-1}. Among them, rearrangement $\mathbf{4}^+ \rightarrow \mathbf{2}^+$ via $\mathbf{1}^+$ is the most competitive energetically.

There are two plausible pathways for rearrangement $\mathbf{5}^+ \rightarrow \mathbf{8}^+$. Both entail the same mechanism: ring opening followed by 1,2-H shift involving nonclassical structures $\mathbf{8b}^+$ and $\mathbf{8c}^+$. The pathway proceeding via $\mathbf{5}-\mathbf{8a}^+$ has a ΔE_b of 127 kJ mol^{-1} and the ΔE_b for the other pathway involving $\mathbf{5}-\mathbf{8b}^+$ is 6 kJ mol^{-1} larger. The calculated ΔH_{r0} for dissociation **16** → H_2S^+ + HCC is in line with the pattern of the ionic fragment (*m*/*z* 34) shown in high-energy angle-resolved CAD spectrum.[3]

Acknowledgment. S.W.C. acknowledges the use of computer time at the National Center for Supercomputing Application of the University of Illinois at Champaign-Urbana. K.C.L. and W.K.L. thank the Computer Services Center of The Chinese University of Hong Kong for generous allocation of computer time on the SGI Origin 2000 High Performance Server.

References and Notes

(1) Eberlin, M. N.; Majumdar, T. K.; Cooks, R. G. *J. Am. Chem. Soc*. **1992**, *114*, 2884.
(2) Traldi, P.; Hamdan, M.; Paradisi, C. *J. Am. Chem. Soc*. **1990**, *112*, 4774.
(3) Cooks, R. G.; Mabud, Md. A.; Horning, S. R.; Jiang, X.-Y.; Paradisi, C.; Traldi, P. *J. Am. Chem. Soc.* **1989**, *111*, 859.
(4) Caserio, M.; Kim, J. K. *J. Am. Chem. Soc.* **1983**, *105*, 6896.
(5) Paradisi, P.; Scorrano, F.; Daolio, S.; Traldi, P. *Org. Mass Spectrom.* **1984**, *19*, 198.
(6) Rodriquez, C. F.; Hopkinson, A. C. *Can. J. Chem*. **1987**, *65*, 1209.
(7) Csizmadia, I. G.; Bernardi, F.; Lucchini, V.; Modena, G. *J. Chem. Soc., Perkin Trans. 2* **1977**, 542.
(8) Kollman, P.; Nelson, S.; Rothenberg, S. *J. Phys. Chem.* **1978**, *82*, 1403.
(9) Mó, O.; de Paz, L. G.; Yáñez, M. *J. Phys. Chem.* **1987**, *91*, 6484.
(10) Lien, M. H.; Hopkinson, A. C. *J. Am. Chem. Soc.* **1988**, *110*, 3788.
(11) Csizmadia, I. G.; Duke, A. J.; Lucchini, V.; Modena, G. *J. Chem. Soc., Perkin Trans. 2* **1974**, 1808.
(12) Lias, S. G.; Bartmess, E.; Lieman, J. F.; Holmes, J. L.; Levin, R. D.; Mallard, W. G. *J. Phys. Chem. Ref. Data* **1988**, *17*, Suppl. 1.
(13) Mallard, W. G.; Linstrom, P. J. *NIST Chemistry WebBook*; National Institutes of Standards and Technology: Gaithersburg, MD, Nov. 1998 (http://webbook.nist.gov).
(14) Wiberg, K. B.; Cheeseman, J. R.; Ochterski, J. W.; Frisch, M. J. *J. Am. Chem. Soc.* **1995**, *117*, 6535.
(15) Chiu, S.-W.; Cheung, Y.-S.; Ma, N. L.; Li, W.-K.; Ng, C. Y. *J. Mol. Struct. (THEOCHEM)* **1998**, *452*, 97.
(16) Chiu, S.-W.; Cheung, Y.-S.; Ma, N. L.; Li, W.-K.; Ng, C. Y. *J. Mol. Struct. (THEOCHEM)* **1999**, *468*, 21.
(17) Curtiss, L. A.; Raghavachari, K.; Trucks, G. W.; Pople, J. A. *J. Chem. Phys.* **1991**, *94*, 7221.
(18) Chiu, S.-W.; Lau, K.-C.; Li, W.-K.; Ma, N. L.; Cheung, Y.-S. Cheung; Ng, C. Y. *J. Mol. Struct. (THEOCHEM)* **1999**, *490*, 109.
(19) Jarzecki, A. A.; Davidson, E. R. *J. Phys. Chem. A* **1998**, *102*, 4742.
(20) Chiu, S.-W.; Cheung, Y.-S.; Ma, N. L.; Li, W.-K.; Ng, C. Y. *J. Mol. Struct. (THEOCHEM)* **1997**, *397*, 87.
(21) Lau, K. C.; Li, W.-K.; Ng, C. Y.; Chiu, S.-W. *J. Phys. Chem. A* **1999**, *103*, 3330.
(22) Glaser, R.; Choy, C. C. S. *J. Phys. Chem.* **1994**, *98*, 11379.
(23) Reed, A. E.; Curtiss, L. A.; Weinhold, F. *Chem. Rev.* **1988**, *88*, 899.
(24) Curtiss, L. A.; Raghavachan, K.; Pople, J. A. *J. Chem. Phys.* **1993**, *98*, 1293.
(25) Buzek, P.; Schleyer, P. V.; Vanchik, H.; Mihalic, Z.; Gauss, J. *Angew. Chem., Int. Engl.* **1994**, *33*, 448.
(26) Borden, W. T.; Iwamura, H.; Berson, J. A. *Acc. Chem. Res*. **1994**, *27*, 109.
(27) Hund, F. *Z. Phys*. **1928**, *51*, 759.
(28) Curtiss, L. A.; Raghavachari, K.; Redfern, P. C.; Rassolov, V.; Pople, J. A. *J. Chem. Phys.* **1998**, *109*, 7764.
(29) Hegarty, D.; Robb, M. A. *Mod. Phys.* 1979, *38*, 1795.
(30) Eade, R. H. E.; Robb, M. A. *Chem. Phys. Lett.* **1981**, *83*, 362.
(31) Ochsenfeld, C.; Kaiser, R. I.; Lee, Y. T.; Head-Gordon, M.; *J. Chem. Phys.* **1999**, *110*, 9982.
(32) Ruscic, B.; Berkowitz, J. *J. Chem. Phys.* **1993**, *98*, 2568.
(33) Asmus, K.-D. *Acc. Chem. Res.* **1979**, *12*, 436.
(34) Asmus, K.-D.; Bahenemann, D.; Fischer, Ch.-H.; Veltwisch, D. *J. Am. Chem. Soc.* **1979**, *101*, 5322.
(35) Illies, A. J.; Livant, P.; McKee, M. L. *J. Am. Chem. Soc.* **1988**, *110*, 7980.
(36) Clark, T. *J. Am. Chem. Soc.* **1988**, *110*, 1672.
(37) Belloni, J.; Marignier, J. L.; Katsumura, Y.; Tabata, Y. *J. Phys. Chem.* **1986**, *90*, 4014.
(38) Shustorovich, E. *J. Am. Chem. Soc.* **1978**, *100*, 7513.
(39) Pross, A.; Radom, L. *J. Comput. Chem.* **1980**, *1*, 295.
(40) Davidson, E. R.; Borden, W. T. *J. Phys. Chem.* **1983**, *87*, 4783.
(41) Paldus, J.; Cizek, J. *J. Chem. Phys.* **1970**, *52*, 2919.
(42) Ayala, P. Y.; Schlegel, H. B. *J. Chem. Phys.* **1998**, *108*, 7560.
(43) Barnes, L. A.; Lindh, R. *Chem. Phys. Lett.* **1994**, *223*, 207.
(44) Crawford, T. D.; Stanton, J. F.; Allen, W. D.; Schaefer, H. F. *J. Chem. Phys.* **1997**, *107*, 10626.
(45) Stang, P. J. *Chem. Rev.* **1978**, *78*, 383.
(46) Likhotvorik, I. R.; Brown, D. W.; Jones, M. Jr. *J. Am. Chem. Soc.* **1994**, *116*, 6175.
(47) Fahie, B. J.; Leigh, W. J. *Can. J. Chem.* **1989**, *67*, 1859.
(48) Walsh, R.; Wolf, C.; Untiedt, S.; de Meijere, A. *J. Chem. Soc., Chem. Commun.* **1992**, 421.
(49) Jursic, B. S. *Int. J. Quantum Chem*. **1999**, *72*, 571 and references therein.
(50) Cheung, Y.-S.; Li, W.-K.; Ng, C. Y. *J. Mol. Struct. (THEOCHEM)* **1995**, *339*, 25.
(51) Carsky, P.; Hubak, E. *Theor. Chim. Acta* **1991**, *80*, 407.
(52) Gill, P. M. W.; Wong, M. W.; Nobes, R. H.; Radom, L. *Chem. Phys. Lett.* **1988**, *148*, 541.
(53) Gill, P. M. W.; Radom, L. *Chem. Phys. Lett.* **1986**, *132*, 16.
(54) Chase, M. W., Jr. *NIST-JANAF Thermochemical Tables*, 4th ed.; *J. Phys. Chem. Ref. Data* **1998**, *9*, 1−1951.
(55) Tsang, W. In *Energetics of Organic Free Radicals*; Martinho Simoes, J. A., Greenberg, A., Liebman, J. F., Eds.; Blackie Academic and Professional: London, 1996; pp 22−58.
(56) Ervin, K. M.; Gronert, S.; Barlow, S. E.; Gilles, M. K.; Harrison, A. G.; Bierbaus, V. M.; DePuy, C. H.; Lin, W. C. *J. Am. Chem. Soc*. **1990**, *112*, 5750.
(57) Janousek, B. K.; Brauman, J. I.; Simons, J. *J. Chem. Phys.* **1979**, *71*, 2057.
(58) Bartmess, J. E.; Scott, J. A.; McIver, R. T., Jr. *J. Am. Chem. Soc.* **1979**, *101*, 6047.
(59) Hunter, E. P.; Lias, S. G. Evaluated Gas-Phase Basicities and Proton Affinities of Molecules: An Update; *J. Phys. Chem. Ref. Data* **1998**, *27*, 413−656.